

Dehydrocostuslactone disrupts signal transducers and activators of transcription 3 through up-regulation of suppressor of cytokine signaling in breast cancer cells

Po-Lin Kuo,^{1,3,4} Wen-Chiu Ni,² Eing-Mei Tsai,^{2,3,5} and Ya-Ling Hsu^{2,3}

¹Institute of Clinical Medicine and ²Graduate Institute of Medicine, College of Medicine, ³Center of Excellence for Environmental Medicine, Kaohsiung Medical University, Kaohsiung, Taiwan; and ⁴Department of Medical Research, ⁵Department of Obstetrics and Gynecology, Kaohsiung Medical University Hospital, Kaohsiung, Taiwan

Abstract

This study investigates the anticancer effect of dehydrocostuslactone (DHE), a plant-derived sesquiterpene lactone, on human breast cancer cells. DHE inhibits cell proliferation by inducing cells to undergo cell cycle arrest and apoptosis. DHE suppresses the expression of cyclin D, cyclin A, cyclin-dependent kinase 2, and cdc25A and increases the amount of p53 and p21, resulting in G₀/G₁-S phase arrest in MCF-7 cells. In contrast, DHE caused S-G₂/M arrest by increasing p21 expression and chk1 activation and inhibiting cyclin A, cyclin B, cdc25A, and cdc25C expression in MDA-MB-231 cells. DHE induces up-regulation of Bax and Bad, down-regulation of Bcl-2 and Bcl-XL, and nuclear relocation of the mitochondrial factors apoptosis-inducing factor and endonuclease G. We also found that DHE inhibits survival signaling through the Janus tyrosine kinase-signal transducer and activator of transcription-3 signaling by increasing the expression of suppressors of cytokine signaling (SOCS)-1 and SOCS-3. Reduction of SOCS-1 and SOCS-3 expression by small interfering RNA inhibits DHE-mediated signal transducer and activator of transcription-3 inhibition, p21 up-regulation, and cyclin-dependent kinase 2 blockade, supporting the hypothesis that DHE inhibits cell cycle progression and cell death through SOCS-1 and SOCS-3. Significantly, animal studies have re-

vealed a 50% reduction in tumor volume after a 45-day treatment period. Taken together, this study provides new insights into the molecular mechanism of the DHE action that may contribute to the chemoprevention of breast cancer. [Mol Cancer Ther 2009;8(5):1328–39]

Introduction

Breast cancer is one of the most common human malignancies and the second leading cause of cancer-related deaths in women, and its incidence in the developing world is on the rise (1). Different treatment strategies have been proposed with the intention to reduce mortality rates, including surgery and radiotherapy and adjuvant chemo- or hormone-therapies (2). However, breast cancer is particularly challenging because it is highly resistant to radiation and conventional chemotherapeutic agents, and this resistance is associated with a poor prognosis for this metastatic disease, particularly in hormone receptor-positive breast cancer (1, 3). About 30% to 40% of women with this form of cancer will develop metastasis and eventually die from this disease (4). Novel therapeutic agents are therefore needed to deal with the increasing incidence of human breast cancer.

Janus tyrosine kinase-signal transducer and activator of transcription (JAK/STAT) signaling has been shown to participate in various cellular processes, including immune function, cell proliferation, differentiation, survival, motility, and apoptosis (5, 6). Abnormal activation of JAK/STAT3 signaling has been seen in multiple tumors including breast cancers (5). Binding of specific ligands to cytokines receptors leads to receptor dimerization and cross-activation of receptor-associated JAK kinases, which in turn phosphorylates tyrosine, leading to changes of intercellular parts of receptors and subsequent activation of receptor-associated JAKs, followed by STAT docking and phosphorylation (6, 7). Phosphorylated STAT dimers can bind to STAT-responsive elements in the promoters of various genes, resulting in modulation of their transcriptions (8). Suppressors of cytokine signaling (SOCS) proteins negatively regulate cytokine receptor signaling by several distinct mechanisms (7). The SOCS family has eight members, SOCS-1 to SOCS-7 and cytokine-inducible SH2-containing protein (CIS), which contains a variable amino-terminal region, a central SH2 domain, and a conserved carboxyl-terminal domain, which are designated as the SOCS boxes. SOCSs directly inhibit JAK kinases by binding to the receptor or to the JAK activation loop (7). SOCS proteins compete with STATs for binding sites on the receptor by SH2 domains (8). In addition, SOCS proteins can target the receptor complex and associated signaling proteins for proteasomal degradation through their SOCS boxes, which mediate interactions with elongins B

Received 9/22/08; revised 2/3/09; accepted 2/5/09; published OnlineFirst 4/21/09.

Grant support: National Science Council of Taiwan grant NSC 96-2628-B-041-001-MY3, Kaohsiung Medical University Research Foundation grant KMU-Q098009, and Center of Excellence for Environmental Medicine, Kaohsiung Medical University grant KMU-EM-98-3.

The costs of publication of this article were defrayed in part by the payment of page charges. This article must therefore be hereby marked *advertisement* in accordance with 18 U.S.C. Section 1734 solely to indicate this fact.

Requests for reprints: Ya-Ling Hsu, Graduate Institute of Medicine, College of Medicine, Kaohsiung Medical University, No. 100, Shih-Chuan 1st Road, Kaohsiung 807, Taiwan. Phone: 886-7-312-1101, ext. 6355; Fax: 886-7-321-0701. E-mail: hsuyl326@gmail.com

Copyright © 2009 American Association for Cancer Research.

doi:10.1158/1535-7163.MCT-08-0914

and C to recruit an E3 ubiquitin ligase complex (9, 10). Evidence is accumulating which indicates that suppression of SOCS- and SOCS-3 gene expression has been described for various solid tumors and hematologic malignancies (11–14). Those studies have revealed that SOCS proteins are implicated in the regulation of cellular proliferation and apoptosis (11, 12). Therefore, restoration of SOCS expression may be a potential treatment for cancer therapy (11).

Dehydrocostuslactone (DHE; Supplementary Fig. S1A),⁶ a plant-derived sesquiterpene lactone, was extracted from medicinal tropical plants *Saussurea lappa* and *Aucklandia lappa* (15, 16). *S. lappa* is one of the most important traditional Chinese crude drugs for the treatment of abdominal pain and indigestion (15). DHE has been found to possess antifungal and antimycobacterial activity (17) and has also been reported to exhibit a cytotoxic effect against HepG2, OVCAR-3, and HeLa cell lines (15). However, the anticancer effect and mechanism of DHE in human breast cancer remain unknown. This present study sought (a) to determine the antiproliferative effect of DHE *in vitro* and *in vivo*, (b) to assay the effect of DHE on cell cycle progression and apoptosis, (c) to investigate JAK/STAT3 signaling as potential molecular targets of DHE, and (d) to establish the up-regulation of SOCS-1 and SOCS-3 to augment apoptosis by DHE in human breast cancer.

Materials and Methods

Cell Cultures

MCF-7 (ATCC HTB-22) and H184B5F5/M10 were cultured in DMEM with nonessential amino acids, 0.1 mmol/L sodium pyruvate, 10 µg/mL insulin, and 10% FCS. MDA-MB-231 (ATCC HTB-26) cells were cultured in RPMI 1640 supplemented with 10% FCS, 0.1 mg/mL streptomycin, and 100 units/mL penicillin (Life Technologies, Inc.).

Cell Proliferation and Clonogenic Assays

Cells were plated in 96-well culture plates (1×10^4 per well) and treated with vehicle alone (0.1% DMSO) and various concentrations of DHE for 48 h. Inhibition of cell proliferation was measured by 2,3-bis[2-methoxy-4-nitro-5-sulfophenyl]-2*H*-tetrazolium-5-carboxanilide inner salt (XTT) assay as described previously (18). To determine long-term effects, cells (1,000 per well) were treated with DHE at various concentrations for 3 h. After being rinsed with fresh medium, cells were allowed to form colonies for 14 d and then were stained with crystal violet (0.4 g/L; Sigma).

Cell Cycle Analysis

To determine cell cycle distribution analysis, 5×10^5 cells were plated in 60-mm dishes and treated with vehicle alone (0.1% DMSO) and various concentrations of DHE for 6 h. After treatment, the cells were collected by trypsinization, fixed in 70% ethanol, washed in PBS, resuspended in PBS

containing 1 mg/mL RNase and 50 µg/mL propidium iodide, incubated in the dark for 30 min at room temperature, and analyzed with a flow cytometer (Becton Dickinson and Co.). The data were analyzed using Multicycle software (Phoenix Flow Systems).

Apoptosis Assay

Cells (1×10^6) were treated with vehicle alone (0.1% DMSO) and 8 µg/mL DHE for the indicated times, and then both adherent and suspension cells were collected by trypsinization and centrifugation ($300 \times g$, 10 min). Pellets were lysed by DNA lysis buffer [10 mmol/L Tris (pH 7.5), 400 mmol/L EDTA, and 1% Triton X-100] and then centrifuged. The supernatant obtained was incubated overnight with proteinase K (0.1 mg/mL) and then with RNase (0.2 mg/mL) for 2 h at 37°C. After extraction with phenol-chloroform (1:1), the DNA was separated in 2% agarose gel and visualized by UV after staining with ethidium bromide. Apoptotic cells were quantitatively assessed by the terminal deoxynucleotidyl transferase-mediated dUTP nick end labeling (TUNEL) method, which examines DNA strand breaks during apoptosis by using BD ApoAlert DNA Fragmentation Assay kit as described previously (18).

Subcellular Fractionation/Immunoblot

Subcellular fractionation was done using Nuclear Extract kit (Active Motif) and Cytoplasmic Extraction Reagents kit (BioVision) according to the manufacturers' instructions. Immunoblot analysis was carried out as described previously (18).

Cdk2 Kinase and Immunoprecipitation Assays

Cells were treated with DHE for the indicated times and then harvested. Cell lysates (800 µg of total protein) were incubated with 5 µg of anti-cyclin-dependent kinase (cdk)-2 and 30 µL of protein A-agarose beads (Santa Cruz Biotechnology) for 6 h at 4°C. Association of p21 with cdk2 was detected by incubating the blots with anti-p21 antibodies (Santa Cruz Biotechnology).

For kinase assays, the beads were incubated in 40 µL of kinase reaction buffer [25 mmol/L Tris (pH 7.5), 5 mmol/L β-glycerolphosphate, 2 mmol/L DTT, 0.1 mmol/L Na₃VO₄, 10 mmol/L MgCl₂, 200 µmol/L ATP] containing Rb-C fusion protein (Cell Signaling) for 30 min at 30°C. The reaction was stopped by boiling in sampling buffer. Antibodies against phospho-threonine protein were used to assess the phospho-Rb (Cell Signaling) levels (19).

Immunocytochemistry

After treatment, cells were fixed with methanol, blocked with 5% bovine serum albumin, and stained with apoptosis-inducing factor (AIF) or endonuclease G (Endo G) monoclonal antibody (1:100; Santa Cruz Biotechnology) followed by FITC-conjugated antibody. Nuclear staining was done with 4',6-diamidino-2-phenylindole. The stained cells were then analyzed with a fluorescence microscope (Nikon Eclipse TE 300) at $\times 20$ magnification.

Luciferase Reporter Assays

The pSTAT3-Luc promoter reporter plasmid (Panomics, Inc.) and *Renilla* luciferase reporter vector (pRL-TK;

⁶ Supplementary material for this article is available at Molecular Cancer Therapeutics Online (<http://mct.aacrjournals.org/>).

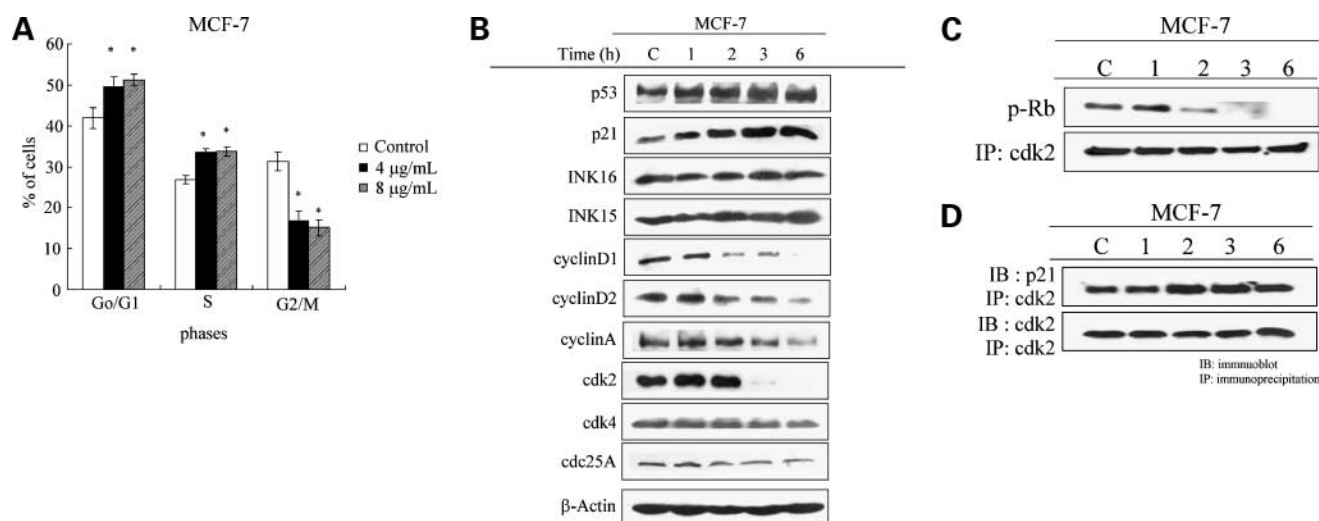


Figure 1. DHE inhibited cell cycle progression in MCF-7 at the G₀/G₁-S phase. **A**, DHE blocked cell cycle progression at the G₀/G₁-S phase in MCF-7. Cells were treated with vehicle and DHE for 6 h, and cell cycle distribution was assessed by flow cytometry. **B**, effect of DHE in G₀/G₁-S regulatory molecules in MCF-7. The cell cycle-related expression levels of 8 $\mu\text{g/mL}$ DHE-treated cancer cells were determined by immunoblot. **C** and **D**, effect of DHE on cdk2 activity (**C**) and the association of p21 and cdk2 (**D**). Cells were treated with 8 $\mu\text{g/mL}$ DHE for the indicated times, then cdk2 activity was assessed by *in vitro* kinase assay (Cdk2 activity reflects the degree of Rb phosphorylation). The interaction of cdk2 and p21 was measured by immunoprecipitation. Results shown are representative of three independent experiments. *, $P < 0.05$, between the control and DHE-treated groups (one-way ANOVA with Dunnett's test post hoc).

Promega) were cotransfected into cells using Lipofectamine 2000. The cells were treated with or without DHE for 6 h and then harvested for luciferase activity assay. The *Renilla* luciferase vector was used as an internal control, and luciferase activity was measured in the cellular extracts using a dual-luciferase reporter assay system (Promega).

Chromatin Immunoprecipitation Assay

Cells were stimulated with 8 $\mu\text{g/mL}$ DHE for the indicated times. A total of 2.5×10^7 cells were used per immunoprecipitation reaction. Cells were cross-linked with 1% formaldehyde for 20 min at room temperature, then terminated by addition of 0.125 mol/L glycine. Cells were subsequently harvested and lysates prepared. The lysates were immunoprecipitated with STAT3 antibody (Santa Cruz Biotechnology). The differential binding of STAT3 to the region -920 to -773 of the survivin promoter was analyzed by PCR. The sequences of the PCR primers used are as follows: forward primer, 5'-CCAAAGCAGAGGACACAC-3'; reverse primer, 5'-GGCCACTACCGTGATAAG-3' (20).

Reverse Transcription-PCR

RNA isolation was done using the TRIzol reagent (Invitrogen). cDNA was prepared using an oligo (dT) primer and reverse transcriptase (Promega) following standard protocols. Primers used in these experiments were as follows: survivin, 5'-GCCTTCCTTAAAGGC-CATC-3' and 5'-AACCTTCCCAGACTCCACT-3'; GAPDH, 5'-ACCACAGTCCATGCCATCAC-3' and 5'-TCCACCACCCTGTTGCTGTA-3'. The primers of Bcl-2 family proteins used ApoPrimer Bcl-2 Set (Takara). After reverse transcription, the cDNA product was amplified by PCR with 3 units of Taq DNA polymerase (Promega) and 2.5 mmol/L Mg²⁺, following standard protocols, at an annealing temperature of 55°C.

In vivo Tumor Xenograft Study

Female nude mice [6 wk old; BALB/cA-nu (nu/nu)] were purchased from the National Science Council Animal Center (Taipei, Taiwan) and maintained in pathogen-free conditions. MDA-MB-231 cells were injected s.c. into the flanks of these nude mice ($5 \times 10^6/200 \mu\text{L}$), and tumors were allowed to develop for ~30 d until they reached a size of ~100 mm³, when treatment was initiated. Thirty mice were randomly divided into two groups. The mice in the DHE-treated group were i.p. injected daily with DHE in a clear solution containing 25% polyethylene glycol (10 mg/kg of body weight) in a volume of 0.2 mL. The control group was treated with an equal volume of vehicle. After transplantation, tumor size was measured with calipers, and tumor volume estimated according to the following formula: tumor volume (mm³) = $L \times W^2/2$, where L is the length and W is the width. The tumor-bearing mice were sacrificed after 45 d.

Statistical Analysis

Data were expressed as means \pm SD. Statistical comparisons of the results were made using ANOVA. Significant differences ($P < 0.05$) between the means of control and DHE-treated cells or two test groups were analyzed by Dunnett's test.

Results

DHE Inhibits Cell Growth and Decreases Colony Formation in Both MCF-7 and MDA-MB-231 Cells

We first confirmed the inhibitory effects of DHE on cell proliferation in two human breast cancer cell lines, MCF-7 (estrogen receptor positive, p53 wild type, model of early-stage breast cancer) and MDA-MB-231 (estrogen receptor negative, p53 mutation, model of more advanced stage breast cancer), by using XTT and colony

formation assays. As shown in Supplementary Fig. S1B,⁶ DHE inhibited cell proliferation not only in early-stage breast cancer MCF-7 but also in more advanced stage MDA-MB-231 cancer cells when the cells were exposed to graded doses (0.65–5 $\mu\text{g}/\text{mL}$) for 48 hours. The IC_{50} values of DHE were $3.7 \pm 0.11 \mu\text{g}/\text{mL}$ for MDA-MB-231 and $3.2 \pm 0.23 \mu\text{g}/\text{mL}$ for MCF-7. In contrast, the proliferation inhibitory effect of DHE on H184B5F5/M10 normal mammary epithelial cells was not significant at the same concentrations as on tumor cells.

The DHE potency was determined by using colony formation assay to measure the reproductive integrity of MCF-7 and MDA-MB-231 cells treated with vehicle alone and with various concentrations of DHE for 3 hours. As shown in Supplementary Fig. S1C,⁶ the clonogenic ability of MCF-7 and MDA-MB-231 cell lines decreased. Compared with untreated cancer cells, the colony formation of MCF-7 decreased to 17.3%, whereas survival of MDA-MB-231 cells decreased to 7% after treatment with DHE at 8 $\mu\text{g}/\text{mL}$. In contrast, the colony formation inhibitory effect of DHE on H184B5F5/M10 cells was not significant at the same concentrations as on tumor cells.

To examine the effect of DHE on cell proliferation, we also evaluated the amount of proliferating cell nuclear antigen. The results showed that DHE decreased the amount of proliferating cell nuclear antigen in both MCF-7 and MDA-MB-231 (Supplementary Fig. S1D).⁶

Differential Responses of MCF-7 and MDA-MB-231 Cells to DHE-Mediated Cell Cycle Arrest

The antiproliferative effects of many anticancer or chemopreventive agents are closely linked to their ability to cause cell cycle arrest (3). We therefore raised the question of whether the DHE-mediated inhibition of breast cancer cells was due to cell cycle arrest. Treatment of MCF-7 cells with DHE (4 and 8 $\mu\text{g}/\text{mL}$) for 6 hours increased the percentage of cells in the G_0/G_1 -S phase in MCF-7 cells (Fig. 1A). Using immunoblot analysis, we assessed the effect of DHE treatment on the protein expression of cyclin D1, cyclin D2, cyclin A, cdk2, cdk4, cdc25A, INK family protein, p53, and p21, which are known to regulate the G_0/G_1 -S phases. Treatment of MCF-7 cells with DHE resulted in decreases in the protein expression of cyclin D1, cyclin D2, cyclin A, cdk2, and cdc25A (Fig. 1B). DHE treatment also increased p53 and p21 expression. However, DHE failed to affect cdk4, INK15, and INK16 in MCF-7 at any of the examined time points (Fig. 1B).

We next determined the effect of DHE on MDA-MB-231 cells. Exposure of MDA-MB-231 cells to DHE increased the population of cells in S- G_2/M and decreased the ratio of cells in G_0/G_1 (Fig. 2A). In addition, DHE treatment resulted in a time-dependent decrease in the protein expression of cyclin A, cyclin B, cdk2, cdc25A, cdc25C, and cdc2 in MDA-MB-231 cells (Fig. 2B). One hour of DHE treatment also increased phosphorylation of chk1

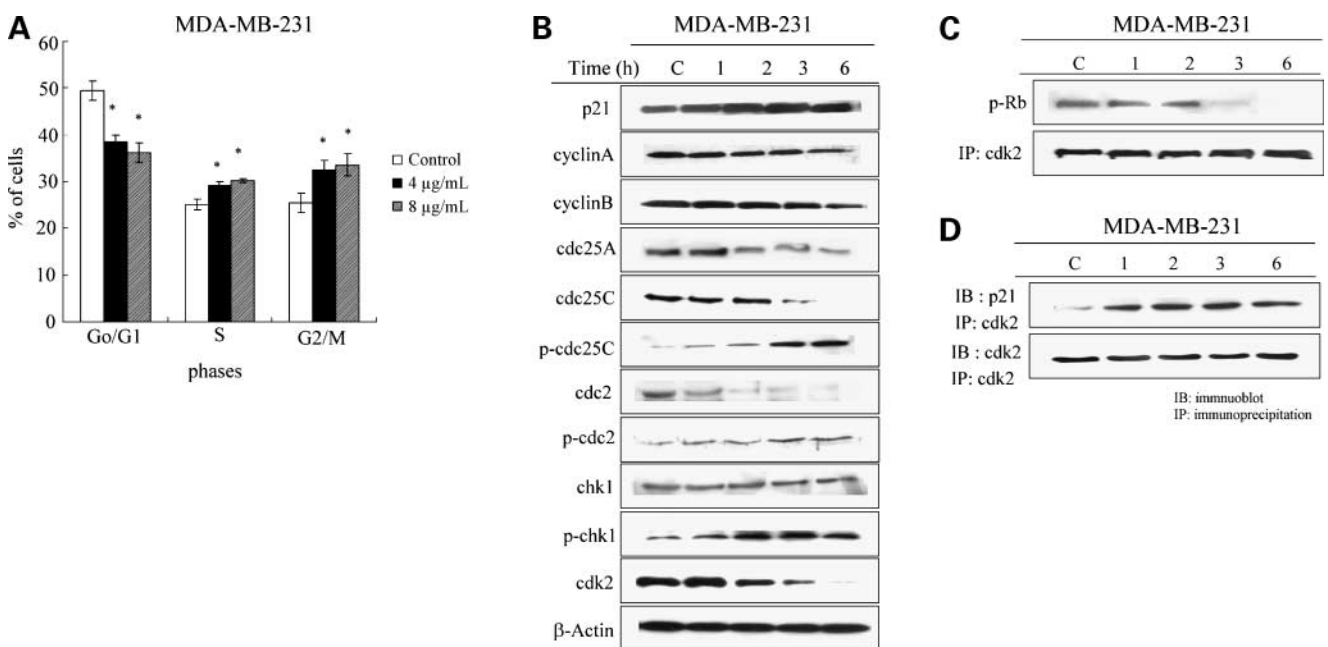


Figure 2. DHE inhibited cell cycle progression in MDA-MB-231 cells at S- G_2/M phase. **A**, effect of DHE on cell cycle distribution in MDA-MB-231 cells. Cells were treated with vehicle and DHE for 6 h, and cell cycle distribution was assessed by flow cytometry. **B**, effect of DHE on the S- G_2/M -related factors in MDA-MB-231 cells. The cell cycle-related expression levels of 8 $\mu\text{g}/\text{mL}$ DHE-treated cancer cells were determined by immunoblot. **C** and **D**, effect of DHE on cdk2 activity (**C**) and the association of p21 and cdk2 (**D**). Cells were treated with 8 $\mu\text{g}/\text{mL}$ DHE for the indicated times, then cdk2 activity was assessed by *in vitro* kinase assay (Cdk2 activity reflects the degree of Rb phosphorylation). The interaction of cdk2 and p21 was measured by immunoprecipitation. Results shown are representative of three independent experiments. *, $P < 0.05$, between the control and DHE-treated groups (one-way ANOVA with Dunnett's test post hoc).

and inactive phospho-cdc25C (Ser216) as well as phospho-cdc2 (Tyr15). Moreover, DHE treatment also increased the expression of cdk inhibitor p21 in MDA-MB-231 cells (Fig. 2B).

Because DHE treatment caused an S-phase arrest in both cancer cell lines, we further assessed the activity of cdk2 and the interaction of p21 and cdk2. As shown in Figs. 1C and 2C, DHE treatment decreased the activity of cdk2 in both cancer cell lines. DHE also increased the association of p21 and cdk2 in a time-dependent manner in both MCF-7 and MDA-MB-231 cells (Figs. 1D and 2D).

DHE Induces Apoptosis by Caspase-Independent Pathways

To address whether the antiproliferative effect of DHE is also associated with the induction of cell death, the apoptotic effects of DHE in both cancer cell lines were determined by DNA electrophoresis and TUNEL assay. DHE induced apoptosis in both cancer cell lines, as determined by DNA fragmentation assay, at a concentration of 8 $\mu\text{g}/\text{mL}$ (Supplementary Fig. S2A).⁶ A quantitative evaluation was also made using TUNEL to detect DNA strand breaks. Compared with vehicle-treated cells,

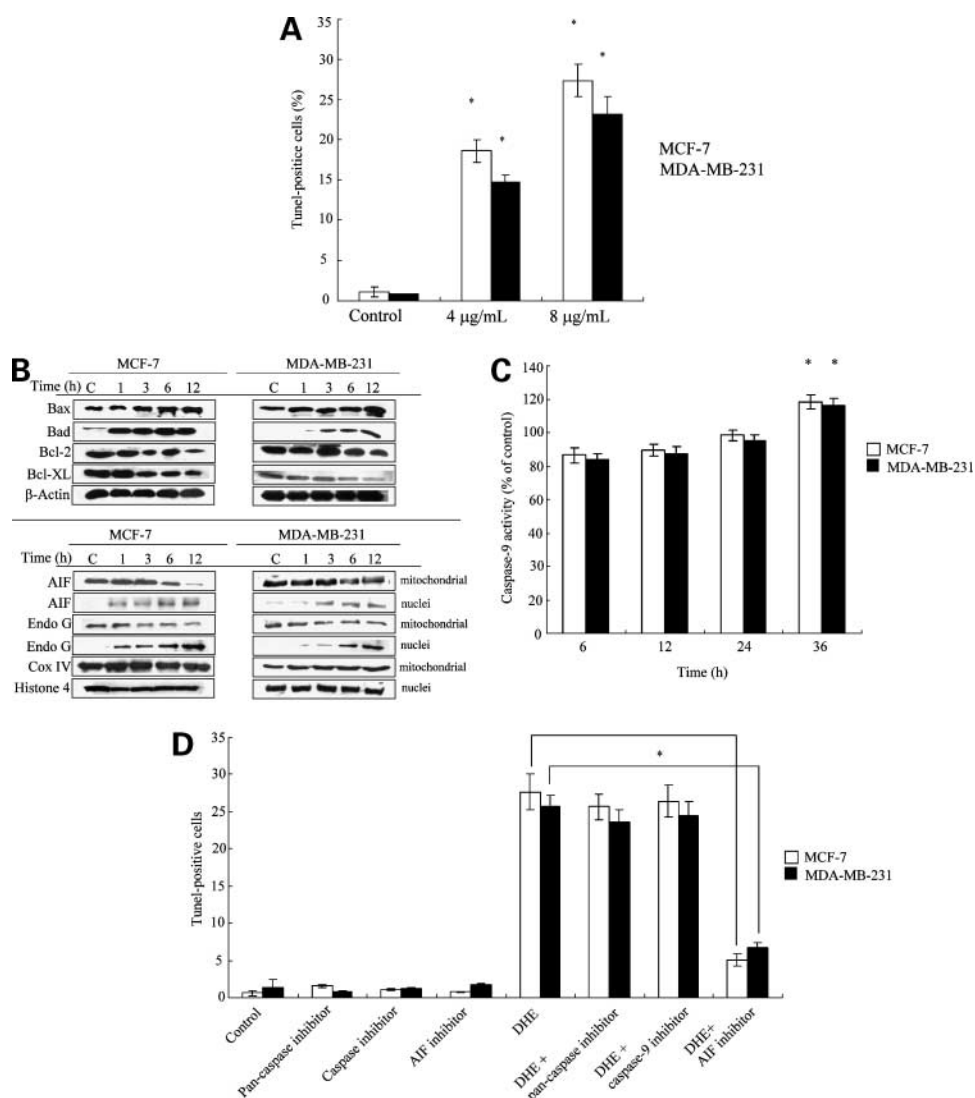


Figure 3. DHE induced apoptosis by caspase-independent pathways. **A**, effects of DHE on apoptosis in MCF-7 and MDA-MB-231 cells, as determined by TUNEL assay at 48 h of treatment. Cells were treated with 4 and 8 $\mu\text{g}/\text{mL}$ of DHE for 48 h. The TUNEL-positive cells were examined by flow cytometry. **B**, effect of DHE on Bcl-2 family proteins and AIF/Endo G translocation. Cells were treated with 8 $\mu\text{g}/\text{mL}$ DHE for the indicated times, then various expressions of proteins were assessed by immunoblot. **C**, DHE increased the activation of caspase-9. Cells were treated with 8 $\mu\text{g}/\text{mL}$ DHE for the indicated times, then caspase-9 activity was assessed by caspase-9 activity kit. **D**, effects of caspase-9, pan-caspase, and AIF inhibitors on DHE-induced apoptosis. Cells were preincubated with *N*-phenylmaleimide (50 $\mu\text{mol}/\text{L}$), z-VAD-fmk (20 $\mu\text{mol}/\text{L}$), or LEHD-CHO (20 $\mu\text{mol}/\text{L}$) for 1 h before the addition of DHE for an additional 48 h. The rate of apoptotic cells was assessed by TUNEL. Columns, mean from three independent experiments; bars, SD. *, $P < 0.05$, between the control and DHE-treated groups (one-way ANOVA with Dunnett's test post hoc).

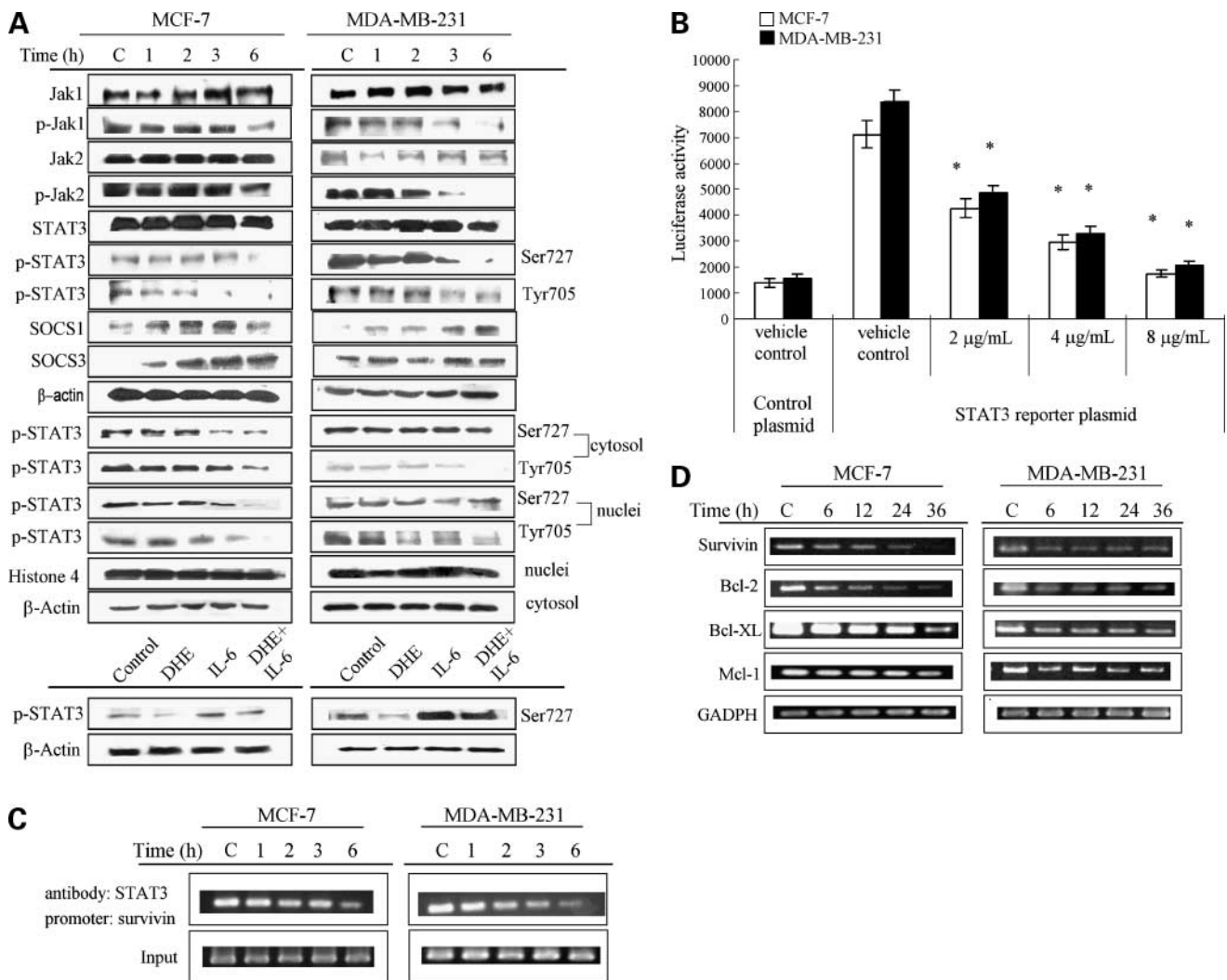


Figure 4. DHE inhibited JAK/STAT3 signaling by up-regulation of SOCS-1 and SOCS-3. **A**, effect of DHE on the expression and translocation of JAK/STAT3. Cells were treated with 8 μ g/mL DHE for the indicated times. In interleukin-6 (IL-6) stimulation experiment, cells were pretreated with 8 μ g/mL DHE for 1 h. Interleukin-6 (60 ng/mL) was added and incubated for 30 min. The expression of various proteins was assessed by immunoblot. DHE decreased the transcriptional activity of STAT3 (**B**) and the recruitment of STAT3 on survivin promoter (**C**). Cells were cotransfected with control plus *Renilla* luciferase or STAT3 reporter plasmid plus *Renilla* luciferase and treated with DHE for 6 h. Luciferase activity was measured in the cellular extracts using a dual-luciferase reporter assay system. The binding of STAT3 on surviving promoter was assessed by chromatin immunoprecipitation. **D**, DHE decreased the mRNA expression of STAT3 target genes. The various amounts of mRNA were determined by reverse transcription-PCR. Results shown are representative of three independent experiments. *, $P < 0.05$, between the control and DHE-treated groups (one-way ANOVA with Dunnett's test post hoc).

8 μ g/mL DHE induced 27.3% and 23.1% apoptotic cells in MCF-7 and MDA-MB-231 cells at 48 hours, respectively (Fig. 3A).

We further confirmed mitochondrial apoptotic pathways triggered by DHE in both cancer cell lines by examining the expression of Bcl-2 family proteins. Immunoblot analysis showed that treatment of MCF-7 and MDA-MB-231 cells with DHE increased Bax and Bad protein levels (Fig. 3B). In contrast, DHE decreased Bcl-2 and Bcl-XL levels, which led to an increase in the proapoptotic/antiapoptotic Bcl-2 ratio. The exposure of MCF-7 and MDA-MB-231 cells to DHE slightly increased caspase-9 activity (Fig. 3C). However, neither pan-caspase inhibitor *z*-VAD-fmk nor caspase-9 specific inhibitor

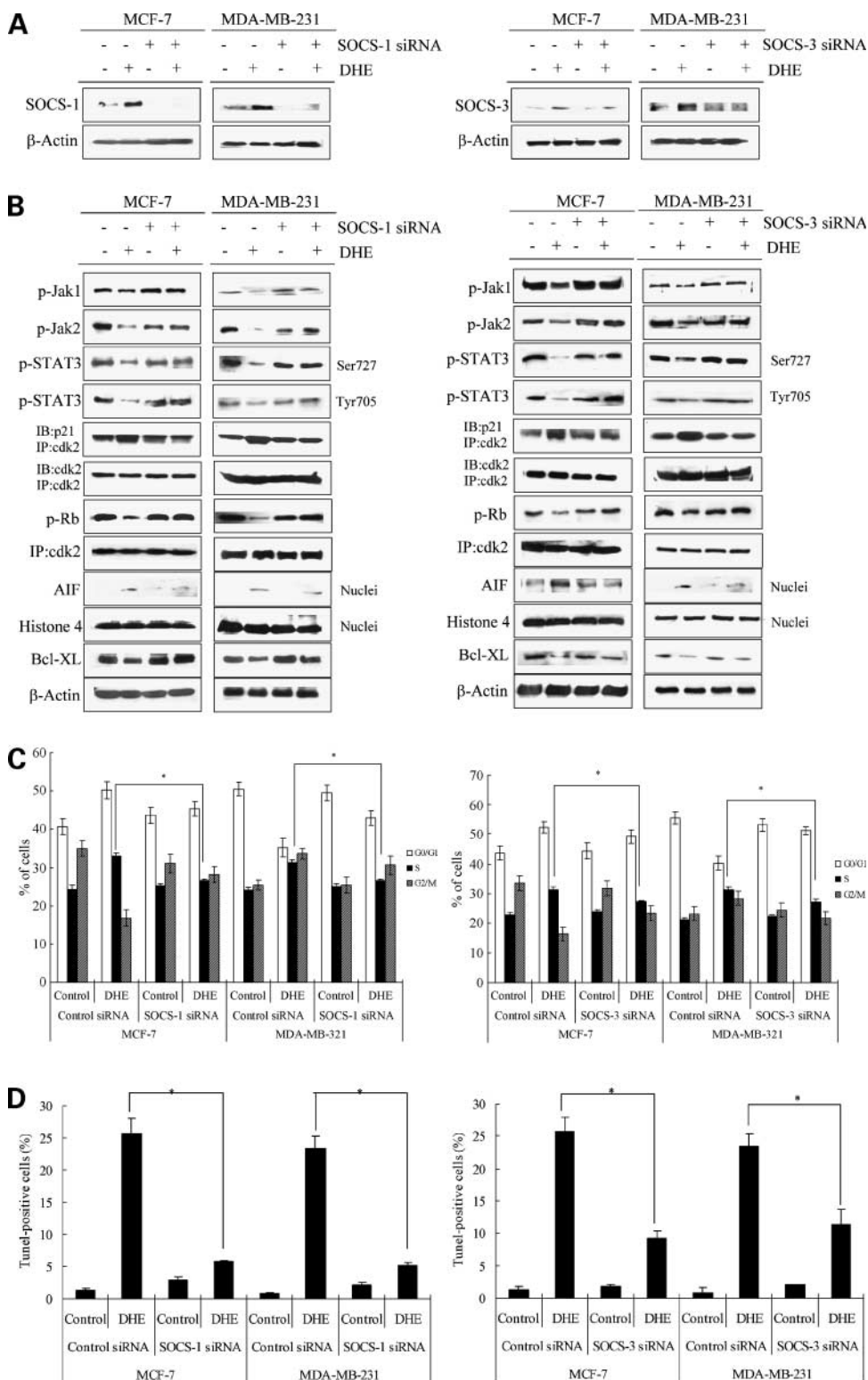
LEHD-CHO caused significant changes in DHE-mediated cell apoptosis (Fig. 3D).

Given the failure of caspase inhibitors to halt DHE-induced cell death, we next explored whether DHE triggers caspase-independent apoptotic events and, in particular, if it induces the release of the AIF and Endo G from the mitochondria into the nuclei. Immunoblot data showed that whereas control cells showed a lack of nuclear expression of AIF and Endo G, DHE treatment induced demonstrable translocation of AIF and Endo G to the nuclei (Fig. 3B). These results were also verified by immunohistochemistry data (Supplementary Fig. S2B and C).⁶ Specific inhibition of AIF by chemical inhibitor *N*-phenylmaleimide (50 μ mol/L) also inhibited DHE-mediated apoptosis (Fig. 3D).

DHE Inhibits the JAK/STAT3 Signaling Pathway

We investigated whether JAK/STAT3, which has been reported to be constitutively activated in and to increase the progression of breast cancer (5), is involved

in DHE-mediated apoptosis in the two cancer cell lines. DHE treatment of cells was found to cause a reduction in the amount and phosphorylation of JAK1 and JAK2 (Fig. 4A). Similarly, DHE caused a significant time-



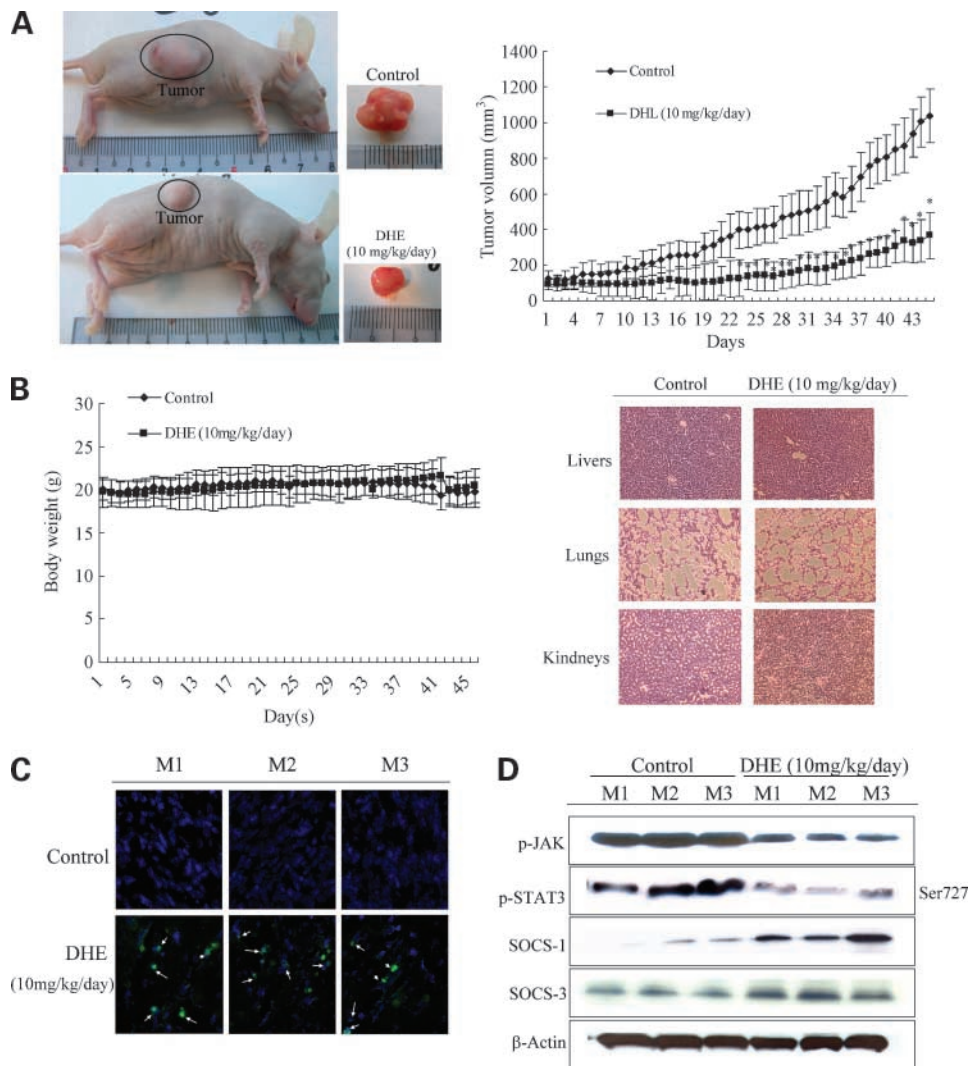


Figure 6. DHE decreased the growth and induced apoptosis of MDA-MB-231 xenografts. **A**, representative tumor-bearing nude mice (45th day of treatment), tumors from the control and DHE-treated groups, and the mean tumor volume measured at the indicated number of days after implant. Animals bearing preestablished tumors ($n = 15$ per group) were dosed daily for 45 d with i.p. injections of DHE (10 mg/kg/d) or vehicle. During the 45-d treatment, tumor volumes were estimated by measurements taken with external calipers (mm³). **B**, means of body weight and tissue sections of livers, lungs, and kidneys in vehicle- and DHE-treated mice. **C**, DHE was shown to induce apoptosis in MDA-MB-231 xenograft, as determined by TUNEL assay. Tumor sections of nude mice were harvested after 45-d dosing. Apoptosis of tumor section was assessed by TUNEL assay, and the cell nuclei were stained with 4',6-diamidino-2-phenylindole. Numerous apoptotic cells (arrows) were observed in DHE-treated groups. **D**, expression of JAK/STAT-3 and SOCSs. The levels of various proteins of tumor section were assessed by immunoblot analysis. *, $P < 0.05$, between the control and DHE-treated groups (one-way ANOVA with Dunnett's test post hoc).

dependent decrease in the phosphorylation (Tyr705 and Ser727) of STAT3, a downstream target of JAK1 and JAK2 proteins in both cancer cell lines. In addition, DHE treatment also decreased phospho-STAT3 in both cytoplasmic and nuclear fractions (Fig. 4A). In contrast,

DHE increased the expressions of SOCS-1 and SOCS-3 in a time-dependent manner (Fig. 4A). DHE was also shown to inhibit STAT3 activation (phosphorylation) induced by interleukin-6 in both cancer cell lines (Fig. 4A). These results suggest that DHE not only inhibits constitutive STAT3

Figure 5. The role of SOCS-1 and SOCS-3 on DHE-mediated cell cycle arrest and apoptosis. **A**, inhibition effect of SOCS-1 and SOCS-3 ON-TARGET SMARTpool siRNA. Cells were transfected with control oligonucleotide and ON-TARGET SMARTpool SOCS-1 and SOCS-3 siRNA using Lipofectamine 2000. After 96-h transfection, cells were treated with 8 μ M DHE for 3 h. The expression of SOCS-1 and SOCS-3 was assessed by immunoblot. The effect of SOCS-1 and SOCS-3 inhibition on JAK/STAT3 activation and cell cycle-related factors, Bcl-XL expression, and AIF nuclear translocation (**B**); cell cycle (**C**); and apoptosis (**D**) in DHE-treated cells. Control, SOCS-1, or SOCS-3 siRNA-transfected cells were treated with DHE for the indicated times (6 h for cell cycle distribution, 3 h for p21 cdk2 activity and p21/cdk2 interaction, 12 h for Bcl-XL expression and AIF translocation, and 48 h for apoptosis assay) after 96-h transfection. The expressions of various proteins were assessed by immunoblot, and apoptosis was determined by TUNEL. Data shown are representative of three independent experiments. *, $P < 0.05$, between the control and DHE-treated groups (one-way ANOVA with Dunnett's test post hoc).

activation but also aborts interleukin-6–induced STAT3 phosphorylation.

DHE-mediated inhibition of STAT3 was additionally confirmed by plasmid reporter assay. As shown in Fig. 4B, STAT3 was constitutively activated in MCF-7 and MDA-MB-231 cells. However, DHE completely inhibited STAT3 activation after 6 hours of exposure. Next, the differential recruitment of STAT3 on survivin promoter was examined by chromatin immunoprecipitation assays. As shown in Fig. 4C, DHE caused a significant reduction in the binding of STAT3 on the survivin promoter in both cancer cell lines.

STAT3 has been shown to increase the transcriptions of cell survival-related proteins including Bcl-2, Bcl-XL, Mcl-1, and survivin (7). Therefore, we investigated whether DHE inhibits the transcriptional activity of these genes. Treatment of cells with DHE was examined for STAT3 response gene products by reverse transcription-PCR. As shown in Fig. 4D, DHE caused a significant reduction in the amount of Bcl-2, Bcl-XL, Mcl-1, and survivin mRNA.

The Role of SOCS-1 and SOCS-3 in DHE-Induced Cell Cycle and Apoptosis

Because SOCS is an inhibitor of STAT3, and STAT3 promotes cell cycle progression and cell survival resulting in cancer development (7, 10), we next addressed the role of SOCS-1 and SOCS-3 in DHE-mediated cell cycle and apoptosis by specific genetic knockdown. Transfection of MCF-7 and MDA-MB-231 cells with SOCS-1 and SOCS-3 small interfering RNA (siRNA) reduced the basal levels and DHE-mediated up-regulation of SOCS-1 and SOCS-3 in both cancer cell lines (Fig. 5A). In addition, DHE-mediated STAT3 inhibition was significantly attenuated in SOCS-1 and SOCS-3 knockdown cells compared with the vector control cells. These data support the hypothesis that DHE decreases STAT3 activation through SOCS-1 and SOCS-3 up-regulation (Fig. 5B).

A previous study has reported that inhibition of the JAK/STAT3 pathway causes a delay of cell cycle progression by increasing p21 expression and subsequently decreases cdk2 activity (21). We assessed the roles of SOCS-1 and SOCS-3 in the distribution of cell cycle- and S-phase-related molecules after DHE treatment. As shown in Fig. 5C, selective genetic inhibition of SOCS-1 and SOCS-3 abrogated DHE-mediated S-phase arrest in both cell lines (Fig. 5C). SOCS-1 and SOCS-3 inhibition also caused a significant inhibition of DHE-mediated interaction of p21 with cdk2, as well as a decrease in cdk2 activity (Fig. 5B). These data suggest that SOCS-1 and SOCS-3 are involved in DHE-mediated cell cycle arrest.

Similarly, specific knockdown SOCS-1 and SOCS-3 expression by siRNA also decreased DHE-mediated Bcl-XL down-regulation and AIF nuclear translocation (Fig. 5B). Inhibition of SOCS-1 and SOCS-3 also reduced apoptotic cell death in DHE-treated cells (Fig. 5D). These results suggest that SOCS-1 and SOCS-3 may also play key roles in DHE-mediated apoptosis.

DHE Inhibits Tumor Growth in Nude Mice

We further used animal experiments to determine whether DHE decreases the growth of MDA-MB-231 xenografts *in vivo* and if DHE inhibits JAK/STAT3 signaling in tumors *in vivo*. As shown in Fig. 6A, the average tumor volume in mice treated with 10 mg/kg/d DHE was statistically significantly lower compared with vehicle-treated control mice, starting from day 23 to day 45. Tissue sections of lungs, livers, and kidneys, as well as the mean body weight of the DHE-treated group, did not indicate any significant differences between vehicle- and DHE-treated mice (Fig. 6B). These results indicate that DHE administration at 10 mg/kg/d dose significantly inhibits MDA-MB-231 xenograft growth without causing any side effects to the mice.

To gain insights into the mechanism of DHE-mediated suppression of MDA-MB-231 xenograft growth, we compared the induction of apoptosis and the phosphorylation of JAK/STAT3 proteins in tumors from control and DHE-treated mice. As shown in Fig. 6C, tumors from the DHE-treated mice exhibited a markedly higher amount of apoptosis compared with control tumors. In addition, the phosphorylation of JAK and STAT3 was relatively lower in tumors from DHE-treated mice when compared with the control tumors (Fig. 6D). These results indicate that DHE-mediated apoptosis and JAK/STAT3 inhibition in cultured cells and *in vivo* are correlated.

Discussion

The important findings from the present study are that DHE inhibits proliferation of human breast cancer cell lines and that this effect may be the consequence of cell cycle arrest and caspase-independent apoptosis. In addition, *in vivo* studies showed that i.p. injections of DHE significantly decrease the growth of MDA-MB-231 cells (Fig. 6). Moreover, our data also show that DHE treatment did not produce any overt signs of toxicity *in vivo*, nor did it exhibit any significant toxicity on normal breast cells *in vitro* (Fig. 6B; Supplementary Fig. S1C),⁶ which suggests that DHE possesses selectivity between normal and cancer cells.

Loss of cell cycle checkpoint controls that regulate the passage of cells through the cell cycle is a hallmark of cancer progression (22). The cell cycle regulatory pathway may represent a useful target for drug and gene therapy approaches (23, 24). Our results show that DHE delays the transition of MCF-7 cells from the G₀/G₁-S phase, whereas it induces an S-G₂/M phase arrest in MDA-MB-231 cells (Figs. 1A and 2A). When cells enter the cell cycle from G₁ phase, cyclin D1 is synthesized and is associated with its catalytic partner, cdk4, depending on mitogenic stimulation (22). Down-regulation of cyclin D increases the duration of the G₁ phase (22). On the other hand, cyclin B/cdc2 heterodimeric complex plays a critical role during the G₂ phase. During the G₂ phase, cyclin B/cdc2 complex remains inactive by phosphorylation of cdc2 at Tyr15. Cdc25C, a phosphatase, is necessary for the G₂-M

transition that can remove the phosphate group of cdc2 at Tyr15 and then restore the function of cyclin B/cdc2 complex, resulting in M-phase entrance (18, 23, 25). By means of immunoblot data, we found that DHE causes cyclin D1 and cyclin D2 degradation. Up-regulation of p53 and its downstream target p21 was observed in MCF-7 cells (Fig. 1B). These results were consistent with the cell cycle analysis data, which showed that DHE causes a G₀/G₁ phase arrest in MCF-7 cells (Fig. 1A). In contrast, the present study also reveals that DHE decreases the expression of cyclin B, cdc25A, cdk2, cdc25C, and cdc2, whereas it increases the phosphorylation of chk1 (activation) and cdc2 (inactivation), as well as phospho-cdc25C (inactivation), in MDA-MB-231 cells (Fig. 2B). DHE induces phosphorylation of cdc25C (Ser216) through chk1 activation and remains cdc25C inactive. Further downstream, inactivated cdc2 was not dephosphorylated by cdc25C. Therefore, cdc2 accumulated in an inactive phosphorylated state (Tyr15), resulting in MDA-MB-231 cells that were unable to move through the mitotic phase (Fig. 2A and B). Therefore, we suggest that DHE may prove to be a valuable tool for inhibition of cell cycle progression through different action models in different breast cancer cell lines.

In addition to regulation of cdk complex assembly and function, cell cycle progression is also controlled by several regulatory molecules such as tumor suppressor gene *p53*. *p53* is crucial in the induction of cell cycle arrest and apoptosis in human cells following DNA damage or other kinds of cellular stress such as hypoxia, nucleotide depletion, or activated oncogenes (25, 26). MCF-7 cells have a normal tumor suppression gene, *p53*, whereas in MDA-MB-231 a major protein of the *p53* gene is mutated and accompanied by the absence of *p53* transcriptions and *p53* protein (27). Our results show that DHE delays MCF-7 cell transition from the G₀/G₁-S phase, whereas it induces an S-G₂/M phase arrest in MDA-MB-231 cells. Furthermore, immunoblot data also show that DHE increases the expression of *p53* in MCF-7 cells. This implies that *p53* may be the major influence that causes different levels of responsiveness of the two cell lines on initiation of cell cycle checkpoint.

S-phase arrest has been observed in several cellular systems treated with various chemical agents, including gemcitabine, etoposide, deoxyribonucleotide triphosphate, meformin, and selenocysteine (28). DNA damage could activate the intra-S checkpoint, which allows DNA repair and the G₂-M cell cycle arrest to prevent cell mitosis in the presence of DNA damage. The mechanism of S-phase arrest is more poorly understood than that of G₀/G₁ and G₂-M arrest. It has been reported that S-phase cell cycle arrest occurs with the loss of cdk2 activity due to up-regulation of p21 and reduced formation of active cyclin A/Cdk2 complex (29). Another report has suggested that phosphorylation of checkpoint kinase leads to degradation of cdc25A and deactivation of cyclin E/A-cdk2 complex (29, 30). We found that DHE caused cyclin A and cdc25A degradation (Figs. 1B and 2B). In addition, DHE also reduced cdk2 activity (Figs. 1C and 2C) and function by in-

creasing the association of p21 and cdk2 in both cell lines (Figs. 1D and 2D). Thus, we believe that DHE blocks S-phase progression through cdk inhibitor up-regulation and cyclin inhibition pathways.

Mitochondria play an important role in apoptotic signaling pathways. Severe apoptogenic factors are released from the mitochondrial intermembrane space to the cytosol or nuclei, resulting in apoptotic cell death (31, 32). Among the mitochondrial factors known to be involved in apoptosis, AIF and Endo G seem to be highly conserved evolutionarily and are normally confined to the mitochondrial intermembrane space (32). Mature AIF and Endo G are known to translocate to the nucleus in response to apoptogenic stimuli, and overexpression of AIF and Endo G induces peripheral chromatin condensation, dissipation of the mitochondrial transmembrane potential, and DNA fragmentation (33, 34). Bcl-2 family members are the major controllers of mitochondrial membrane permeability. The Bcl-2 subfamily (Bcl-2 and Bcl-XL) functions to inhibit apoptosis, whereas the Bax subfamily (Bax and Bak) and the BH3-only subfamily (Bad, Bid, Bik, Bim, and Bmf) promote apoptosis (31, 32). DHE treatment results in a significant increase of Bax and Bad expression and a decrease of Bcl-2 and Bcl-XL, suggesting that changes in the ratio of proapoptotic and antiapoptotic Bcl-2 family proteins might contribute to the apoptosis-promoting activity of DHE (Fig. 3B). Our findings also showed that DHE treatment causes an activation of caspase-9, an effector caspase known to be activated in mitochondria in a caspase-dependent manner. However, our findings also show that pretreatment of the cells with pan-caspase inhibitors or specific caspase-9 inhibitor failed to block DHE-induced apoptosis (Fig. 3D). These results suggest that DHE-induced apoptosis may not require caspase activation. In contrast, our results also show that both AIF and Endo G are progressively released from the mitochondria to the nuclei after incubation of human breast cancer cells with DHE (Fig. 3B). Moreover, pretreatment of MCF-7 and MDA-MB-231 cells with AIF inhibitor completely prevented DHE-mediated apoptosis (Fig. 3D), further suggesting that the cooperation of AIF and Endo G plays a crucial role in DHE-induced apoptosis. Previous studies have documented the fact that serious nuclear DNA damage can initiate AIF/Endo G translocation and subsequently induce apoptosis, as indicated in *Rhus verniciflua* chloroform-methanol fraction and zoledronic acid-mediated cell death (35, 36). Moreover, apoptotic nuclear DNA damage can cause S-phase arrest and initiate AIF/Endo G translocation (36). Because DHE triggers the intra-S DNA checkpoint, this suggests that DHE may cause nuclear DNA damage and then initiate AIF/Endo G-mediated apoptosis.

STAT family proteins are activated by multiple receptor and nonreceptor tyrosine kinases in response to various cytokines, hormones, and growth factors (6, 37). Growing evidence has implicated STAT1, STAT3, and STAT5 in oncogenic pathways, particularly STAT3 (6, 7). Activated STAT3 in turn signals to a variety of key downstream molecules, including Bcl-XL, Bcl-2, Mcl-1, and survivin, the

consequence of which is cell death inhibition and promotion of cell survival (6, 7, 38). Hyperactivation of JAK/STAT3 results in altering the response of tumor cells to chemotherapy (39, 40), and recent studies have indicated that inhibition of the JAK/STAT3 pathway has consistently been associated with triggering of apoptosis in cancer (41, 42). Our results show that DHE treatment decreases the activation of JAK1/2, followed by a decrease of STAT3 phosphorylation (Fig. 4A). The inhibitory effects of DHE on JAK/STAT3 are correlated with the loss of DNA binding and transcriptional activity of STAT3 (Fig. 4B and C). In addition, exposure to DHE also reduces the expression of the STAT3 downstream targets including Mcl-1, Bcl-XL, Bcl-2, and survivin (Fig. 4D). These data were further confirmed by decreased recruitment of STAT3 on survivin promoter. These findings indicate that DHE can be an effective inhibitor of JAK/STAT3 signaling.

SOCS proteins inhibit JAK/STAT3 signaling by inactivating JAK or blocking recruitment site for STAT and may also target JAK/STAT3 complex for ubiquitination and degradation (11). The expressions of SOCS-1 and SOCS-3 genes are dysregulated in several solid tumors, causing aberrant activation of cell growth and survival signaling pathways (11–14). SOCS seems to be an important tumor suppressor in cancers. SOCS-1 mimetic, TKip, has been reported to inhibit cellular proliferation and delay S-phase progression in human prostate cancer cells (43). Reintroduction of SOCS-1 expression sensitized cells to radiation in glioblastoma cells (11). In addition, inhibition of the JAK/STAT pathway has been reported to induce S-phase arrest by up-regulation of p21 expression (21). Our results show that DHE treatment increases the expression of both SOCS-1 and SOCS-3 (Fig. 4A). The up-regulation of DHE on SOCS-1 and SOCS-3 is correlated with the decrease in the amount of JAK1/2 and phosphorylation of STAT3. These effects are abolished in MCF-7 and MDA-MB-231 cells transfected with SOCS-1 and SOCS-3 siRNA, suggesting that SOCS-1 and SOCS-3 enhancement is the upstream event of JAK/STAT3 inhibition (Fig. 5B). In addition, selective knockdown SOCS-1 and SOCS-3 expression not only decreases DHE-mediated cell cycle arrest but also reduces up-regulation of p21, interaction of p21/cdk2, and cdk2 activity (Fig. 5B and C). Similarly, SOCS-1 and SOCS-3 knockdown by siRNA-based inhibition approach also decreases the effects of DHE on the down-regulation of Bcl-XL and apoptosis (Fig. 5B and D), suggesting that the cooperation of SOCS-1 and SOCS-3, which in turn inhibits JAK/STAT3, plays a crucial role in DHE-induced cell cycle arrest and apoptosis in human breast cancer cells.

In conclusion, our results show for the first time that DHE, a natural product, induces both proliferation inhibition in breast cancer cells through cell cycle blockade and apoptosis. In addition, DHE increases SOCS-1 and SOCS-3 expression, followed by inhibition of the JAK/STAT3 pathway (Supplementary Fig. S3).⁶ More importantly, DHE inhibits tumor cell growth in a MDA-MB-231 xenograft mouse model through induction of apoptosis and is well tolerated.

These results provide the preclinical evidence for the further study of the development of DHE as a potential agent against breast cancer.

Disclosure of Potential Conflicts of Interest

No potential conflicts of interest were disclosed.

References

- Ocaña A, Pandiella A. Identifying breast cancer druggable oncogenic alterations: lessons learned and future targeted options. *Clin Cancer Res* 2008;14:961–70.
- Feuer EJ, Wun LM, Boring CC, Flanders WD, Timmel MJ, Tong T. The lifetime risk of developing breast cancer. *J Natl Cancer Inst* 1993;85:892–7.
- Doyle DM, Miller KD. Development of new targeted therapies for breast cancer. *Breast Cancer* 2008;15:49–56.
- Come SE, Buzdar AU, Ingle JN, et al. Endocrine and targeted manipulation of breast cancer: summary statement for the Sixth Cambridge Conference. *Cancer* 2008;112:673–8.
- Garcia R, Bowman TL, Niu G, et al. Constitutive activation of Stat3 by the Src and JAK tyrosine kinases participates in growth regulation of human breast carcinoma cells. *Oncogene* 2001;20:2499–513.
- Germain D, Frank DA. Targeting the cytoplasmic and nuclear functions of signal transducers and activators of transcription 3 for cancer therapy. *Clin Cancer Res* 2007;13:5665–9.
- Valentino L, Pierre J. JAK/STAT signal transduction: regulators and implication in hematological malignancies. *Biochem Pharmacol* 2006;71:713–21.
- Smirnova OV, Ostroukhova TY, Bogorad RL. JAK-STAT pathway in carcinogenesis: is it relevant to cholangiocarcinoma progression? *World J Gastroenterol* 2007;13:6478–91.
- O'Sullivan LA, Liongue C, Lewis RS, Stephenson SE, Ward AC. Cytokine receptor signaling through the JAK-Stat-Socs pathway in disease. *Mol Immunol* 2007;44:2497–506.
- Elliott J, Johnston JA. SOCS: role in inflammation, allergy and homeostasis. *Trends Immunol* 2004;25:434–40.
- Zhou H, Miki R, Eeva M, et al. Reciprocal regulation of SOCS 1 and SOCS-3 enhances resistance to ionizing radiation in glioblastoma multiforme. *Clin Cancer Res* 2007;13:2344–53.
- Weber A, Hengge UR, Bardenheuer W, et al. SOCS-3 is frequently methylated in head and neck squamous cell carcinoma and its precursor lesions and causes growth inhibition. *Oncogene* 2005;24:6699–708.
- Sutherland KD, Lindeman GJ, Choong DY, et al. Differential hypermethylation of SOCS genes in ovarian and breast carcinomas. *Oncogene* 2004;23:7726–33.
- Niwa Y, Kanda H, Shikauchi Y, et al. Methylation silencing of SOCS-3 promotes cell growth and migration by enhancing JAK/STAT and FAK signalings in human hepatocellular carcinoma. *Oncogene* 2005;24:6406–17.
- Sun CM, Syu WJ, Don MJ, Lu JJ, Lee GH. Cytotoxic sesquiterpene lactones from the root of *Saussurea lappa*. *J Nat Prod* 2003;66:1175–80.
- Li A, Sun A, Liu R. Preparative isolation and purification of costunolide and dehydrocostuslactone from *Aucklandia lappa* Decne by high-speed counter-current chromatography. *J Chromatogr A* 2005;1076:193–7.
- Barrero AF, Oltra JE, Alvarez M, Raslan DS, Saúde DA, Akssira M. New sources and antifungal activity of sesquiterpene lactones. *Fitoterapia* 2000;71:60–4.
- Kuo PL, Chen CY, Hsu YL. Isoobtusilactone A induces cell cycle arrest and apoptosis through reactive oxygen species/apoptosis signal-regulating kinase 1 signaling pathway in human breast cancer cells. *Cancer Res* 2007;67:7406–20.
- Lu G, Seta KA, Millhorn DE. Novel role for cyclin-dependent kinase 2 in neuregulin-induced acetylcholine receptor ϵ subunit expression in differentiated myotubes. *J Biol Chem* 2005;280:21731–8.
- Dasgupta P, Kinkade R, Joshi B, Decook C, Haura E, Chellappan S. Nicotine inhibits apoptosis induced by chemotherapeutic drugs by up-regulating XIAP and survivin. *Proc Natl Acad Sci U S A* 2006;103:6332–7.
- Xiong H, Zhang ZG, Tian XQ, et al. Inhibition of JAK1, 2/STAT3 signaling induces apoptosis, cell cycle arrest, and reduces tumor cell invasion in colorectal cancer cells. *Neoplasia* 2008;10:287–97.

22. Shapiro GI. Cyclin-dependent kinase pathways as targets for cancer treatment. *J Clin Oncol* 2006;24:1770–83.
23. Kuo PL, Hsu YL, Cho CY. Plumbagin induces G₂-M arrest and autophagy by inhibiting the AKT/mammalian target of rapamycin pathway in breast cancer cells. *Mol Cancer Ther* 2006;5:3209–21.
24. Kudo Y, Kitajima S, Ogawa I, Kitagawa M, Miyauchi M, Takata T. Small interfering RNA targeting of S phase kinase-interacting protein 2 inhibits cell growth of oral cancer cells by inhibiting p27 degradation. *Mol Cancer Ther* 2005;4:471–6.
25. Halazonetis TD, Gorgoulis VG, Bartek J. An oncogene-induced DNA damage model for cancer development. *Science* 2008;319:1352–5.
26. Hsu YL, Cho CY, Kuo PL, Huang YT, Lin CC. Plumbagin (5-hydroxy-2-methyl-1,4-naphthoquinone) induces apoptosis and cell cycle arrest in A549 cells through p53 accumulation via c-Jun NH₂-terminal kinase-mediated phosphorylation at serine 15 *in vitro* and *in vivo*. *J Pharmacol Exp Ther* 2006;318:484–94.
27. Toillon RA, Chopin V, Jouy N, Fauquette W, Boilly B, Le Bourhis X. Normal breast epithelial cells induce p53-dependent apoptosis and p53-independent cell cycle arrest of breast cancer cells. *Breast Cancer Res Treat* 2002;71:269–80.
28. Blasina A, Hallin J, Chen E, et al. Breaching the DNA damage checkpoint via PF-00477736, a novel small-molecule inhibitor of checkpoint kinase 1. *Mol Cancer Ther* 2008;7:2394–404.
29. Cheng KY, Noble ME, Skamnaki V, et al. The role of the phospho-CDK2/cyclin A recruitment site in substrate recognition. *J Biol Chem* 2006;281:23167–79.
30. Sexl V, Diehl JA, Sherr CJ, Ashmun R, Beach D, Roussel MF. A rate limiting function of cdc25A for S phase entry inversely correlates with tyrosine dephosphorylation of Cdk2. *Oncogene* 1999;18:573–82.
31. Youle RJ, Strasser A. The BCL-2 protein family: opposing activities that mediate cell death. *Nat Rev Mol Cell Biol* 2008;9:47–59.
32. Orrenius S, Gogvadze V, Zhivotovsky B. Mitochondrial oxidative stress: implications for cell death. *Annu Rev Pharmacol Toxicol* 2007;47:143–83.
33. Lorenzo HK, Susin SA. Therapeutic potential of AIF-mediated caspase-independent programmed cell death. *Drug Resist Updat* 2007;10:235–55.
34. Wang M, Zhang L, Han X, et al. Atiprimod inhibits the growth of mantle cell lymphoma *in vitro* and *in vivo* and induces apoptosis via activating the mitochondrial pathways. *Blood* 2007;109:5455–562.
35. Kook SH, Son YO, Chung SW, et al. Caspase-independent death of human osteosarcoma cells by flavonoids is driven by p53-mediated mitochondrial stress and nuclear translocation of AIF and endonuclease G. *Apoptosis* 2007;12:1289–98.
36. Ory B, Blanchard F, Battaglia S, Gouin F, Rédini F, Heymann D. Zoledronic acid activates the DNA S-phase checkpoint and induces osteosarcoma cell death characterized by apoptosis-inducing factor and endonuclease-G translocation independently of p53 and retinoblastoma status. *Mol Pharmacol* 2007;71:333–43.
37. Lo HW, Hsu SC, Xia W, et al. Epidermal growth factor receptor cooperates with signal transducer and activator of transcription 3 to induce epithelial-mesenchymal transition in cancer cells via up-regulation of TWIST gene expression. *Cancer Res* 2007;67:9066–76.
38. Muto A, Hori M, Sasaki Y, et al. Emodin has a cytotoxic activity against human multiple myeloma as a Janus-activated kinase 2 inhibitor. *Mol Cancer Ther* 2007;6:987–94.
39. Gariboldi MB, Ravizza R, Molteni R, Osella D, Gabano E, Monti E. Inhibition of Stat3 increases doxorubicin sensitivity in a human metastatic breast cancer cell line. *Cancer Lett* 2007;258:181–8.
40. Blaskovich MA, Sun J, Cantor A, Turkson J, Jove R, Sebti SM. Discovery of JSI-124 (cucurbitacin I), a selective Janus kinase/signal transducer and activator of transcription 3 signaling pathway inhibitor with potent antitumor activity against human and murine cancer cells in mice. *Cancer Res* 2003;63:1270–9.
41. Ferrajoli A, Faderl S, Van Q, et al. WP1066 disrupts Janus kinase-2 and induces caspase-dependent apoptosis in acute myelogenous leukemia cells. *Cancer Res* 2007;67:11291–9.
42. Agarwal C, Tyagi A, Kaur M, Agarwal R. Silibinin inhibits constitutive activation of Stat3, and causes caspase activation and apoptotic death of human prostate carcinoma DU145 cells. *Carcinogenesis* 2007;28:1463–70.
43. Flowers LO, Subramaniam PS, Johnson HM. A SOCS-1 peptide mimetic inhibits both constitutive and IL-6 induced activation of STAT3 in prostate cancer cells. *Oncogene* 2005;24:2114–20.